35th Annual International Conference of the IEEE EMBS
Osaka, Japan, 3 - 7 July, 2013

Modeling the Different Sections of the Cardiac Conduction System to Obtain Realistic Electrocardiograms

Lydia Dux-Santoy, Rafael Sebastian, Jose F Rodriguez, Jose M Ferrero

Abstract— **The cardiac conduction system is divided in different sections that play an important role in the cardiac depolarization sequence and define the morphology of the electrocardiogram. In this study we have built several configurations for each section based on anatomical descriptions. The effect of the morphology of the bundle branches, and the density of both Purkinje branches and Purkinje-myocardial junctions (PMJ) has been studied by comparing the pseudo-ECGs obtained with the standard precordial leads of the electrocardiogram. A functional model for the PMJs based on the existence of a conduction adaptation layer is also presented. Simulation results showed a large influence of the His bundle and bundle branches in the pseudo-ECG and helped to elucidate the most appropriate morphology. The functional PMJ model allowed bidirectional communication between the conduction system and the myocardium with realistic transmission delays between both mediums. These results can help to improve current conduction system models and improve depolarization sequences of activation in the ventricles.**

I. Introduction

One of the main players in the fast propagation of the electrical impulse in the heart is the cardiac conduction system (CCS). Understanding the CCS properties is a pre-requisite to properly model the heart electrophysiology, and ultimately build a virtual heart. Knowledge on the different parts of the CCS was expanded by Tawara [1], who described the atrioventricular conduction axis, and Keith [2], who discovered the sinoatrial (SA) node. Studies on the normal activation of the ventricles using micro-electrode mapping have helped to roughly characterize the underlying pathway followed by the electrical impulse originated in the SA node [3], [4]. When the impulse from the SA node reaches the atrio-ventricular node it is delayed. Next, it propagates to the left (LV) and right ventricles (RV) through the His bundle (HB), and finally spreads throughout the Purkinje network (PKN) distributed on the myocardium. The PK fibers are connected to the bulk myocardium at terminal insertion points, known as Purkinje-myocardial junctions (PMJ), from which the electrical wave enters the working myocardium [5]. Due to its relevance, the function of the distal CCS has already been integrated in computer models of the heart by means of cable-like structures that transmit electrical impulses at high speed and are coupled to ventricular tissue [6], [7]. The PMJ are modeled by resistors that connect the cable terminals to one or several myocardial points surrounding them [6], [7], [8]. In general, computational representations include several sections, the HB and bundle branches, the PKN, and the PMJs. The morphology of the HB and the bundle branches is simple, which allows to encode them manually following descriptions from anatomists that have characterized their structure [1], [9], [10]. The majority of algorithms focus primarily in the automatic deployment of the PKN since it is the most complex part, and extends throughout the ventricular endocardium. Modelers use either manual delineations on a segmented ventricular geometry [7], mathematical algorithms that try to mimic observations from histological studies [11], [12], [13], [8], or segmentation from high-resolution images performed on ex-vivo animal specimens [14], [15]. The most distal section of the CCS models requires special connections between the PKN and the ventricular tissue, i.e. PMJs. However, it is still unknown what is the average number of PMJs in the ventricles or their spatial distribution. To overcome this problem, computer models distribute PMJs to mimic the electrical activations sequences observed in electrophysiology experiments [16], [17], or simply allow a random distribution of PMJs.

It is not well defined how each of these three components affects electrical simulations in computer models of the heart that aim to reproduce realistic cardiac electrophysiology. In this study, we analyze the effect of the different sections of the CCS on the electrocardiogram (ECG) using an anatomically-realistic biventricular heart. From an analysis of available information on the anatomy of the HB and bundle branches, we manually build six different models on a segmented biventricular model of the heart to analyze the effect of their structures. In addition, we construct several PKNs with different number of PMJs, and compare the resulting ECGs. Finally, we study the timing of the PMJs in the anterograde and retrograde propagation and present a model that it is able to reproduce physiological behavior.

II. Material and Methods

A. Anatomical Modeling

The anatomically-realistic computational biventricular heart model used in this study was segmented from a human Diffusion Tensor MRI data set [18], [8]. From the segmented surfaces a hexahedral volumetric mesh was built using fixed discretization in voxels with an edge length of $0.5mm$. The total number of nodes and elements required were 1.43 million and 1.29 million, respectively. Each node

L. Dux-Santoy and J.M Ferrero are with the Bioelectronic Group (GBIO) at I3BH, Universitat Politecnica de Valencia, Valencia, Spain. lduxsantoy; cferrero {@i3bh.gbio.es}

R. Sebastian is with Computational Multiscale Physiology Lab (CoMMLab) at the Universitat de Valencia, Valencia, Spain. rafael.sebastian@uv.es

J. Rodriguez is with the Mechanical Engineering Department. Aragon Institute of Engineering Research, University of Zaragoza, Spain jfrodrig@unizar.es

978-1-4577-0216-7/13/$26.00 ©2013 IEEE

was assigned to a region from endocardium (17%), mid-myocardium (41%) and epicardium (42%) to take into account the specific properties of the ionic models [19]. The fiber orientation was estimated from the DTMRI data at the centroid of each element. Finally, several CCS models were integrated into the ventricular model (see Fig. 1 and Table I), which included the HB, PKN and PMJs.

TABLE I
PROPERTIES OF THE HIS BUNDLES MODELED

Ver	RV Morphology		LV morphology		
	NB	location	NB	location	Ref
HB1	2	posteriomedial, anteroapical	4	anterobasal, anterior, midseptal, anteroapical	[20]
HB2	1	anteroapical	2	posterobasal, posteroapical	[3]
HB3	1	anteroapical	3	anterobasal, posterobasal, apical	[10]
HB4	1	anteroapical	3	anteroapical, posteroapical, apical	[10]
HB5	1	anteroapical	3	anteromedial, posteroapical, apical	[10]
HB6	1	anteroapical	2	posterobasal, apical	[21]

Ver: Version
NB: Number of branches

B. Biophysical modeling

The myocardial cells were modeled by the Ten-Tusscher & Panfilov ionic model [22] with specific properties for each cell type. The full His-Purkinje Network was modeled with the Purkinje ionic model by Stewart [23]. The electrical propagation was calculated by means of the monodomain equation, using the operator splitting technique with an adaptive time step with a minimum step of $0.02\ ms$ and a maximum time step of $1ms$. A high order finite element formulation was used, as described in [24], in order to improve numerical efficiency without jeopardizing the accuracy of the solution. The conduction velocity in the PKN was adjusted varying the longitudinal conductivity of this material in order to fit the experimental conduction velocity of $2-3\ m/s$. In particular, the conduction velocity in our CCS was $2.68\ m/s$. Pseudo-ECG calculation was calculated by means of,

$$V_e(r) = -\frac{\gamma}{4\pi}\frac{\sigma_i}{\sigma_e}\int_\Omega \nabla V(r')\cdot\nabla\left[\frac{1}{|r-r'|}\right]d\Omega, \qquad (1)$$

where V_e is the extracelular potential, V the transmembrane potential, $r-r'$ radius vector (distance between each element and the electrode position), and σ_i and σ_e are the intracellular and extracellular conductivities, respectively.

C. CCS modelling

Massing et al. describe both anterior and posterior divisions of the LBB in different positions [10]. In our model the atrio-ventricular node has been placed approximately $2\ mm$ over the base of the ventricular model, in the division between atria and ventricles. In order to study the influence of the anatomy of the HB in the ECG, several anatomical configurations have been considered (see table I). HB definitions have been done considering both anatomical and electrical data available in the literature. These anatomical structures were generated manually. In Fig. 1 three of the HBs delineated are shown.

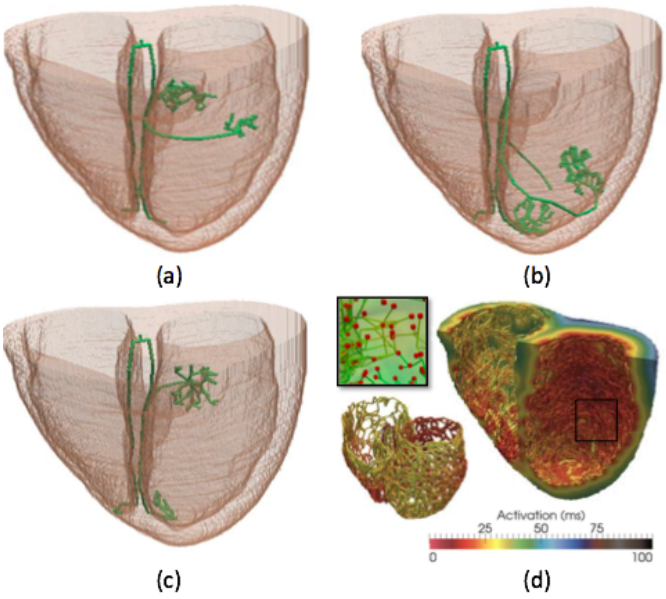

Fig. 1. **His Bundle structures and depolarization sequence. (a) HB4, (b) HB5 and (c) HB6, corresponding to Table I. (d) shows the activation sequences corresponding to HB6 for the PKN and the myocardium. Upper-left detail shows a zoom to the PMJs for a given region.**

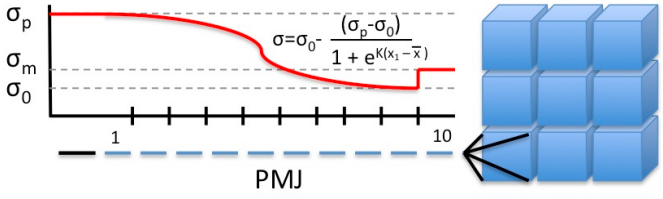

Fig. 2. **Schematic representation of PMJ functional model. The dashed line (blue) at the bottom represents the PMJ, that is connected to the hexahedral nodes (endocardium) by resistances. The continuous red function displays the conductivity transition from $\sigma_p = 0.0068mS/cm$ to $\sigma_0 = 0.0003mS/cm$ along the 10 last sections of the cable model defined by x_1. $\bar{x}$ is the center of the transitional region. σ_p is the conductivity in the Purkinje elements, and $\sigma_m = 0.0013mS/cm$ the conductivity in the myocardium elements. Constant K affects the slope and was set to 100.**

The PKN is constructed by our automatic algorithm [8] that generates a full biventricular PKN from the corresponding endpoints of the bundle branches. First, the algorithm randomly selects the internal endocardial nodes that will form the PKN. Some of these nodes can be predefined as PMJs while the rest are used to establish the connectivity to form a full PKN. Nodes without neighbors in a given radius are marked as PMJs. Finally, the algorithm removes nodes that have not been connected to the PKN. We defined two configurations, a coarse PKN mesh with around 150/300

PMJs for the RV/LV respectively, and a dense PKN mesh with around 450/900 PMJs for the RV/LV, respectively. The structure allowed more looping structures in the LV than the RV, to replicate anatomical observations [25]. Each PMJ was coupled to around 50 nodes in the endocardium by fixed resistances. However, due to the high difference in electrical diffusivity between the PKN and the ventricular tissue the functional model required an adaptation step to allow retrograde conduction, which is important to model certain pathologies such as bundle branch reentrant ventricular tachycardia. We assume that there is a transitional section between each PMJ and the endocardium. In our model it is defined as an intermediate conductivity-adaptation layer. The conductivity transition is done along the last 10 segments of each branch, and it is modeled by a Boltzmann curve (see Fig. 2). Using this approximation and tuning the minimum and maximum conductivities, we could model anterograde and retrograde conduction delays, without including artificial electrical components.

III. Results

For each HB configuration we performed electrical simulations of $5000ms$ with a basic cycle length of $1000ms$ pacing at the AV-node. Following, pseudo-ECGs were calculated using Eq. 1 considering a homogeneous volume between the heart and measuring points or leads. Standard precordial lead positions (V1-V6) were established based on standard torso dimensions and heart position. The disposition of the bundle branches prove to have a great effect on the morphology of the pseudo-ECGs. Fig. 3 shows the pseudo-ECGs for the HB5, that has one of the most complex structure found in the literature. The results for leads V1-V3 showed a low amplitude and incorrect morphologies with double peaks. HB1-HB4 (not shown) presented the worst results with poor correlation with real ECGs. Only HB6 (see Fig. 4) fairly reproduced the morphological properties of the ECG in each lead.

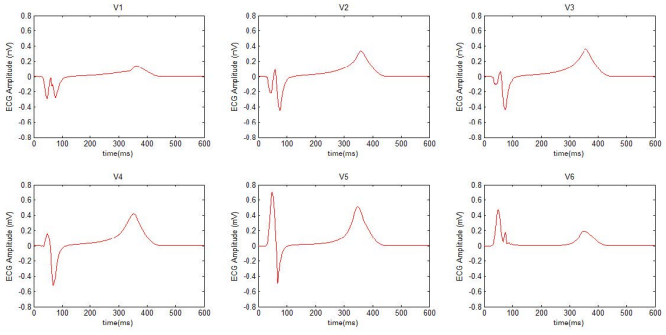

Fig. 3. **Pseudo-ECGs at precordial leads V1-V6 for the HB5 configuration.**

Based on HB6 two different CCS were built with a coarse and a dense number of PMJs. Fig. 4 shows the pseudo-ECG corresponding to both simulations. The morphology of the curves was not affected by the branch and PMJ density, although there were small changes in amplitude and

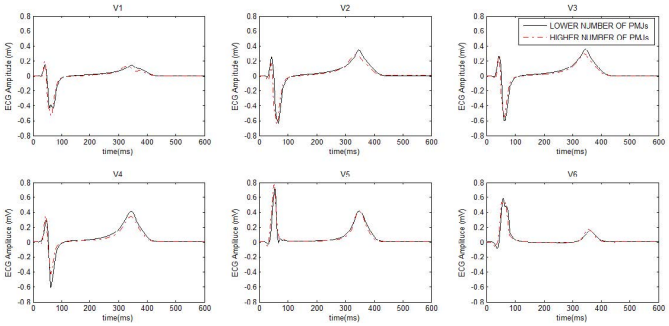

Fig. 4. **Pseudo-ECGs at precordial leads V1-V6 for the HB6 configuration.**

a subtle temporal shifting of the curve. The dense PKN produce smoother pseudo-ECGs which was expected since activation is more synchronized. The total activation time in both simulations was similar, although the dense PKN completed the full activation around 5ms earlier.

Finally, we studied the behavior of the functional connector at the PMJs in 3D. First, a simple resistive element was added to connected each terminal point of the PKN to a set of 4-8 myocardial nodes. The electrical impulse propagated properly in the anterograde direction but failed to conduct impulses originated in the ventricle into the PKN due to the high diffusivity in the CCS. Increasing the number of parallel connections at the terminal points from 8 to 32 myocardial nodes did not help to achieve a retrograde activation. Implementing the adaptation layer in the model using a Boltzmann and the parameters specified in Fig. 2, we obtained a successful retrograde conduction with a delay of $2-3$ms and anterograde conduction delay of $4-5$ms.

IV. Discussion

We have found out that the configuration of the HB is critical in order to obtain a correct sequence of activation and properly shaped pseudo-ECGs. Among the configurations of the HB, the one that included more anatomical details did not produce expected results regarding ventricular activation and synchronization, giving as a result a pseudo-ECG with an awkward morphology. The best morphological results were obtained with a simple HB configuration that only included two LV branches, a posterobasal and an apical branch. Our PKN had larger number of branches and PMJ in LV, considering studies and information by the cardiac anatomist Sanchez-Quintana. In our simulations the pseudo-ECG morphology and amplitude was not significantly modified after doubling the number of nodes of the network in each ventricle. This indicates that there are a number of terminals from which activation does not change its pattern. The coarse PKN model is comparable to that described in [13], where changes in the sequence of the depolarization were small for PKN with more than 150 PMJs. Our results together with known differences between PKN and myocardium properties highlighted the necessity of a special transition layer. Using different values for the PMJ resistance

connectors or increasing the number of parallel connections between PMJs and endocardium did not produced the expected bidirectional asymmetric conduction delays at PMJs. Other authors have solve this problem by including current multipliers, or altering the properties of some currents such as the sodium [26]. Our approach do not requires additional electrical components, producing physiological delays at PMJs in both directions.

The study present several limitations. There is no consistent anatomical data available on the CCS, so its modeling is principally based on observations done in animal hearts and oriented to obtaining adequate simulation results (activation maps, APD maps, pseudo-ECGs). At organ level, we have obtained pseudo-ECGs, which are comparable with real ECGs in morphology but not in amplitude. To obtain more accurate simulated ECGs it is necessary to introduce the heart model in a complete torso model, taking into account different tissue heterogeneities between the heart and the torso. However, the main characteristics of the pseudo-ECG morphology were expected to be comparable to a real ECG.

V. Conclusions

We have modeled several configurations of the HB and PK networks, which have been incorporated in a 3D model of a human subject including the main anatomical and functional components required to perform in-silico electrophysiology studies. Results of simulations with different models of the CCS were tested, showing that the configuration of the HB and its proximal branches is critical in order to obtain right activation patterns and simulated pseudo-ECGs. Surprisingly, better results were obtained with simpler HB models, than with the most anatomically detailed one. The inclusion of a functional model for the PMJs gave the model physiological properties allowing a bidirectional asymmetric electrical propagation. This is required for studies that involve pacing stimulation, or try to reproduce macro-reentrant tachycardia.

VI. Acknowledgments

This study is partly supported by the eTorso project (UV-INVPRECOMP12-80627) from Universitat de Valencia, and the Spanish Ministry of Science and Innovation under the project SAFE-PLAI (TIN2011-28067), and project (UZ2011-TEC-02) from University of Zaragoza.

References

[1] S. Tawara, "Das reizleitungssystem des sugetierherzens. eine anatomisch- histologische studie ber das atrioventricularbndel und die purkinjeschen fden," *Jena, Verlag v. Gustav Fischer*, 1906.

[2] A. Keith and M. Flack, "The form and nature of the muscular connections between the primary divisions of the vertebrate heart." *J Anat Physiol*, vol. 41, no. Pt 3, pp. 172–189, Apr 1907.

[3] D. Durrer, R. T. van Dam, G. E. Freud, M. J. Janse, F. L. Meijler, and R. C. Arzbaecher, "Total excitation of the isolated human heart." *Circulation*, vol. 41, no. 6, pp. 899–912, Jun 1970.

[4] R. J. Myerburg, K. Nilsson, and H. Gelband, "Physiology of canine intraventricular conduction and endocardial excitation." *Circ Res*, vol. 30, no. 2, pp. 217–243, Feb 1972.

[5] J. Tranum-Jensen, A. A. Wilde, J. T. Vermeulen, and M. J. Janse, "Morphology of electrophysiologically identified junctions between purkinje fibers and ventricular muscle in rabbit and pig hearts." *Circ Res*, vol. 69, no. 2, pp. 429–437, Aug 1991.

[6] E. J. Vigmond and C. Clements, "Construction of a computer model to investigate sawtooth effects in the purkinje system," vol. 54, no. 3, pp. 389–399, 2007.

[7] D. Romero, R. Sebastian, B. H. Bijnens, V. Zimmerman, P. M. Boyle, E. J. Vigmond, and A. F. Frangi, "Effects of the purkinje system and cardiac geometry on biventricular pacing: a model study." *Ann Biomed Eng*, vol. 38, no. 4, pp. 1388–1398, Apr 2010.

[8] L. Dux-Santoy, R. Sebastian, J. Felix-Rodriguez, J. M. Ferrero, and J. Saiz, "Interaction of specialized cardiac conduction system with antiarrhythmic drugs: a simulation study." *IEEE Trans Biomed Eng*, vol. 58, no. 12, pp. 3475–3478, Dec 2011.

[9] R. H. Anderson and S. Y. Ho, "The morphology of the cardiac conduction system." *Novartis Found Symp*, vol. 250, pp. 6–17; discussion 18–24, 276–9, 2003.

[10] G. K. Massing and T. N. James, "Anatomical configuration of the his bundle and bundle branches in the human heart." *Circulation*, vol. 53, no. 4, pp. 609–621, Apr 1976.

[11] T. Ijiri, T. Ashihara, T. Yamaguchi, K. Takayama, T. Igarashi, T. Shimada, T. Namba, R. Haraguchi, and K. Nakazawa, "A procedural method for modeling the purkinje fibers of the heart." *J Physiol Sci*, vol. 58, no. 7, pp. 481–486, Dec 2008.

[12] R. Sebastian, V. Zimmerman, D. Romero, and A. Frangi, "Construction of a computational anatomical model of the peripheral cardiac conduction system," *IEEE Trans Biomed Eng*, vol. 58(12), pp. 3479–82, 2011.

[13] R. Sebastian, V. Zimmerman, D. Romero, D. Sanchez-Quintana, and A. Frangi, "Characterization and modeling of the peripheral cardiac conduction system," *IEEE Trans Med Imaging*, vol. 32, pp. 45–55, 2013.

[14] R. Bordas, V. Grau, R. B. Burton, P. Hales, J. E. Schneider, D. Gavaghan, P. Kohl, and B. Rodriguez, "Integrated approach for the study of anatomical variability in the cardiac purkinje system: from high resolution mri to electrophysiology simulation." *Conf Proc IEEE Eng Med Biol Soc*, vol. 2010, pp. 6793–6796, 2010.

[15] R. Bordas, K. Gillow, Q. Lou, I. R. Efimov, D. Gavaghan, P. Kohl, V. Grau, and B. Rodriguez, "Rabbit-specific ventricular model of cardiac electrophysiological function including specialized conduction system." *Prog Biophys Mol Biol*, vol. 107, no. 1, pp. 90–100, Oct 2011.

[16] A. Pollard and R. Barr, "Computer simulations of activation in an anatomically based model of the human ventricular conduction system," *IEEE Trans Biomed Eng*, vol. 38, no. 10, pp. 982–996, 1991.

[17] O. Berenfeld and J. Jalife, "Purkinje-muscle reentry as a mechanism of polymorphic ventricular arrhythmias in a 3-dimensional model of the ventricles." *Circ Res*, vol. 82, no. 10, pp. 1063–1077, Jun 1998.

[18] P. Helm, "A novel technique for quantifying variability of cardiac anatomy application to the dyssynchronous failing heart," Ph.D. dissertation, Johns Hopkins University, 2005.

[19] G. X. Yang, W. Shimizu, and C. Antzelevitch, "Characteristics and distribution of m cells in arterially perfused canine left ventricular wedge preparations," *Circulation*, vol. 98 (18), pp. 1921–1927, 1998.

[20] K. H. W. J. T. Tusscher and A. V. Panfilov, "Modelling of the ventricular conduction system." *Prog Biophys Mol Biol*, vol. 96, no. 1-3, pp. 152–170, 2008.

[21] D. Sanchez-Quintana and S. Y. Ho, "Anatomy of cardiac nodes and atrioventricular specialized conduction system." *Rev Esp Cardiol*, vol. 56, no. 11, pp. 1085–1092, Nov 2003.

[22] K. T. Tusscher and A. V. Panfilov, "Cell model for efficient simulation of wave propagation in human ventricular tissue under normal and pathological conditions." *Phys Med Biol*, vol. 51, no. 23, pp. 6141–6156, Dec 2006.

[23] P. Stewart, O. V. Aslanidi, D. Noble, P. J. Noble, M. R. Boyett, and H. Zhang, "Mathematical models of the electrical action potential of purkinje fibre cells." *Philos Transact A Math Phys Eng Sci*, vol. 367, no. 1896, pp. 2225–2255, Jun 2009.

[24] E. Heidenreich, J. M. Ferrero, M. Doblare, and J. F. Rodriguez, "Adaptive macro finite elements for the numerical solution of monodomain equation in cardiac electrophysiology," *Annals of biomedical engineering*, vol. 38, pp. 2331–2345, 2010.

[25] A. Ansari, S. Y. Ho, and R. H. Anderson, "Distribution of the purkinje fibres in the sheep heart." *Anat Rec*, vol. 254, no. 1, pp. 92–97, Jan 1999.

[26] P. M. Boyle and E. J. Vigmond, "An intuitive safety factor for cardiac propagation." *Biophys J*, vol. 98, no. 12, pp. L57–L59, Jun 2010. [Online]. Available: http://dx.doi.org/10.1016/j.bpj.2010.03.018